



Impacts of Droughts on Biomass Burning Emissions, Air Quality, and Public Health in the Amazon

Leo T.H. Ng¹, Jia Mao², Xueying Liu¹, Shixian Zhai¹, Dominic Fawcett³, Stephen Sitch⁴ and Luiz E.O.C. Aragao^{4,5}, Amos P.K. Tai^{1,6,7}

5 ¹ Department of Earth and Environmental Sciences, Faculty of Science, The Chinese University of Hong Kong, Sha Tin, Hong Kong SAR, China

² Faculty of Applied Sciences, Macao Polytechnic University, Macao 999078, China.

³ Swiss Federal Institute for Forest Snow and Landscape Research WSL, Birmensdorf, Switzerland

⁴ Faculty of Environment, Science, and Economy, University of Exeter, Exeter, United Kingdom

10 ⁵ Earth Observation and Geoinformatics Division, National Institute for Space Research (INPE), São José dos Campos, Brazil

⁶ Institute of Environment, Energy and Sustainability, The Chinese University of Hong Kong, Sha Tin, Hong Kong SAR, China

⁷ State Key Laboratory of Agrobiotechnology, The Chinese University of Hong Kong, Sha Tin, Hong Kong SAR, China

Correspondence to: Amos P.K. Tai (amostai@cuhk.edu.hk)

15 **Abstract.** Wildfires in the Amazon, increasingly influenced by climate variability and anthropogenic activities, pose severe environmental and health challenges. While drought events amplify fire activity and emissions, the cascading effects of droughts and deforestation on air quality and health remain underexplored. This study addresses this gap by combining satellite observations of fire activities with the Global Fire Emissions Database (GFEDv4s) and the chemical transport model, GEOS-Chem High Performance (GCHP) to quantify the impacts of droughts and deforestation on fire emissions, air quality, and health risks from 2010 to 2015. “Fire-on” and “fire-off” simulation reveal that biomass burning dominates dry-season (July–November) air quality, contributing 50% to regional CO and PM_{2.5} and 33% for ozone in non-drought years. These contributions increase to 60–80% for CO and PM_{2.5} and 50% for ozone during drought years. Significant correlations between pollutant levels and drought intensity reflect a climate-driven amplification of fire impacts. Using the Global Exposure Mortality Model (GEMM) and exposure-response relations, we estimate that fire-induced PM_{2.5} and ozone increase premature mortality by 6.0% and 18.6% in non-drought years, which rise to 8.9% and 24.4% during drought years. These findings underscore the critical roles of droughts in exacerbating fire emissions and health risks, even under stable deforestation rates. This study highlights the urgent need for integrated wildfire management and climate adaptation strategies to protect public health and achieve sustainability goals.

1 Introduction

30 Wildfires play a vital role in terrestrial ecosystems by enhancing soil fertility through nutrient cycling (Fuentes-Ramirez et al., 2022), promoting healthy habitats (Elakiya et al., 2023), controlling pest populations (New, 2014; Pausas & Keeley, 2019), and maintaining biodiversity (Keeley et al., 2011; Regan et al., 2011). However, under the influence of climate change and



human activities, the frequency and intensity of wildfires in the Amazon have been increasing over the past few decades. By 2018, about 20% of the Brazilian Amazon forest had been lost due to continuous deforestation, which is often associated with
35 fires (da Cruz et al., 2021). Previous research showed that low precipitation rates during the dry seasons (July to November) can cause water deficits in the Amazon forest, increasing fuel availability and fire risks by providing more dry litter and dead trees (Aragão et al., 2014). These conditions are intensified during drought events, which can be influenced by interannual climate variability regimes such as El Niño Southern Oscillation (ENSO) and Atlantic Multidecadal Oscillation (Marengo et al., 2011; Xu et al., 2020). Among recent drought events (2005, 2010 and 2015) in the Amazon, each was caused by various
40 climate factors and showed unique impacts in both spatial and temporal aspects (Aragão et al., 2007; Jiménez-Muñoz et al., 2016; Marengo et al., 2011). During these events, carbon emissions from the Amazon forest could double, from 0.24 to 0.46 Pg C year⁻¹, and fire-contributed carbon emissions were found to be more than half of those from the old-growth forest deforestation (Aragão et al., 2018; Aragão et al., 2014), turning the Amazon from a carbon sink to a carbon source area (Gatti et al., 2021; van der Laan-Luijkx et al., 2015).

45 Human activities, including agricultural expansion and rapid urbanization, are another dominant contributor to the wildfire occurrences in the southeastern Amazon rainforest and the adjacent Cerrado region. Albert et al. (2023) stated that about 14% of the original forest had been cleared and replaced with agricultural usage, such as cattle ranching and soybean production. The mismanaged pasture fires set by local farmers during the dry season (July to November) often accidentally ignite wildfires
50 in the Amazon and cause forest fragmentation, thereby further enhancing fire activities (Cammelli et al., 2020). According to the annual accumulated deforestation rate statistics of the Instituto Nacional de Pesquisas Espaciais (INPE), the Brazilian Amazon rainforest experienced an average deforestation rate of 18,400 km² per year between 1988 and 2004 (Prodes, 2013). The rapid deforestation rate had raised the awareness of the Brazilian government, leading to the establishment of the Action Plan for Prevention and Control of Deforestation in Amazonia (PPCDAm) in 2004 (Godar et al., 2014). The plan aimed for
55 sustainable development of the Amazon forest and successfully reduced the deforestation rate to 5,820 km² per year between 2010 and 2015 (F. G. Assis et al., 2019; Prodes, 2013).

Recent research has begun to examine the complex interactions between climate, human influences, and wildfire occurrences. A positive feedback between climate change, droughts and wildfire occurrences has been observed in various studies (Aragão
60 et al., 2018; Staal et al., 2020). Studies suggested that cumulative deforestation and future climate change would lead to reduced evapotranspiration and rainfall, exacerbating drought intensity and frequency (Feldpausch et al., 2016; McGregor et al., 2014). More flammable forests with higher fuel availability tend to intensify fires once they start, releasing more carbon, aerosols and other gas species into the atmosphere and amplifying climate change (Cochrane, 2003; Nepstad et al., 2004). Aragão et al. (2018) found that the number of active fires detected by the Moderate Resolution Imaging Spectroradiometer (MODIS) during
65 the third phase of PPCDAm increased by 15% compared to the first phase, even though the deforestation rate was much lower in the third phase. Meanwhile, the monthly cumulative water deficit (CWD) correlated with positive fire anomalies during



drought years (2005, 2010 and 2015), suggesting that drought events have a greater impact on fire occurrences than deforestation.

70 The increasing wildfire occurrences in the Amazon not only affect ecosystem services, but also emit various air pollutants that impact regional climate (Covey et al., 2021; Jacobson, 2014), air quality (Marlier et al., 2020; Werth & Avissar, 2002), and consequently public health (Jacobson, 2014; Marlier et al., 2020). van der Werf et al. (2017) found that 13.4% of global biomass burning emissions are linked to the wildfire events in South America from 1997 to 2016, while 70% of the fire emissions across South America are generated from the Amazon (Butt et al., 2020). These fires emit particulate matter with a diameter of less than 2.5 μm ($\text{PM}_{2.5}$), carbon monoxide (CO), nitrogen oxide ($\text{NO}_x = \text{NO} + \text{NO}_2$), and hundreds of volatile organic compounds (VOCs) (e.g., Jaffe et al., 2022; Permar et al., 2021). NO_x and VOCs can further react in the presence of sunlight to produce ozone (O_3). Therefore, high ozone levels are often observed in the downwind area of wildfires, reflecting regional air pollution problems. $\text{PM}_{2.5}$ emitted from the increasing fires influences the global climate by scattering or absorbing radiation (depending on the component species), altering cloud formation and precipitation patterns (Jiang et al., 2020; Ward et al., 2012). Excessive fires also unnaturally release the carbon stored in the Amazon forest into the atmosphere and reduce its carbon uptake capacity, representing a positive feedback that further enhances global warming (Covey et al., 2021).

The impacts of fire-emitted pollutants on regional public health due to worsening air quality are a substantial concern (Kelly & Fussell, 2015; Pflieger et al., 2023). Among all fire-emitted air pollutants, $\text{PM}_{2.5}$ and ground-level ozone are major concerns due to their pervasiveness and harmful health effects (Sun & Zhou, 2017; Yang & Omaye, 2009). Long-term exposure to $\text{PM}_{2.5}$ has been associated with a wide range of health issues. Epidemiological studies have demonstrated a positive relationship between ambient $\text{PM}_{2.5}$ concentration and the frequency and severity of respiratory ailments, including non-communicable respiratory diseases (NCD) and lower respiratory infections (LRI) (Liang et al., 2020; Pope et al., 2018; Puett Robin et al., 2011; Wong Chit et al., 2015). For ground-level ozone, previous studies found that long-term exposure to ozone causes asthma (Zu et al., 2018), chronic obstructive pulmonary disease (Seltzer et al., 2018) and premature cardiovascular mortality (Jerrett et al., 2013; Turner et al., 2016).

In order to estimate the public health impacts caused by the long-term exposure to $\text{PM}_{2.5}$ and ozone, various models and exposure functions were developed. Burnett et al. (2018) developed the Global Exposure Mortality Model (GEMM), which was used to evaluate premature mortality from NCD and LRI associated with $\text{PM}_{2.5}$ exposure in different age groups. Using the GEMM model, Butt et al. (2020) estimated that around 9,800 premature deaths in the Amazon basin from August to October 2012 were linked to forest fires, as observed $\text{PM}_{2.5}$ concentrations increased from 2 to 30–50 $\mu\text{g m}^{-3}$ during the burning season in the southwestern Amazon region. Vohra et al. (2021) also applied the GEMM model and found approximately 8.9 million deaths worldwide were attributed to long-term exposure to $\text{PM}_{2.5}$ from all sources in 2015. Besides, Jerrett et al. (2009) correlated the American Cancer Society Cancer Prevention Study II with air pollution data to estimate the

contribution of long-term ozone exposure to the premature mortality risk from respiratory causes. A larger-scale epidemiological study involving more participants over a longer period, conducted by Turner et al. (2016), reaffirmed the premature mortality risk from respiratory causes and examined the risk from cardiovascular disease related to long-term ozone exposure. These studies demonstrated the significant increases in premature mortality with enhanced PM_{2.5} and ozone concentration. Consequently, under climate change, the intensified wildfires in the Amazon are expected to exacerbate public health impacts in Brazil with enhanced PM_{2.5} and ozone concentrations.

Recent studies have demonstrated that interannual climate variability including intermittent drought events can cause more frequent and intense fire activity (Aragão et al., 2018; Liu et al., 2024; Silva Junior et al., 2019), emitting various air pollutants that impact regional climate (Covey et al., 2021; Jacobson, 2014), degrade air quality (Marlier et al., 2020; Werth & Avissar, 2002), and consequently pose serious public health risks (Jacobson, 2014; Marlier et al., 2020). While various methods, including remote sensing, statistical modeling and atmospheric chemistry-climate modeling, have been employed to analyze the relationships between fire emissions and air quality (Butt et al., 2020; Cobelo et al., 2023; Nawaz & Henze, 2020), there remains a critical gap in specifically investigating the cascading effects of climatic events and changes such as droughts on air quality by affecting fire emissions. In this study, we combined satellite observations of fire activities and numerical modeling of atmospheric chemistry to estimate the impacts of deforestation and droughts on fire emissions and regional air quality in the Brazilian Amazon and surrounding area during the dry (July-November) season, and the corresponding health impacts from 2010 to 2015. This study not only enhances scientific understanding but also offers insights that may help guide public health policies and environmental management practices that aim to reduce the impacts of fires in the face of climate change. Understanding the dynamics behind climatic factors, fire dynamics, and public health is essential for developing effective strategies to protect public health, alleviate the adverse effects of climate change-driven fire events, and ultimately contribute to the achievement of several Sustainable Development Goals (SDGs).

2 Data and Methods

2.1 Model description

The GEOS-Chem atmospheric chemistry model (www.geos-chem.org), first described by Bey et al. (2001), is an open-source global 3-D atmospheric chemical transport model driven by assimilated meteorological observations from the Goddard Earth Observing System (GEOS) of the NASA Global Modeling and Assimilation Office (GMAO) (<http://acmg.seas.harvard.edu/geos/>). GEOS-Chem includes detailed gas-phase mechanisms for NO_x-VOC-O₃ chemistry and aerosol chemistry for sulfate-nitrate-ammonium aerosols, black carbon (BC), and primary and secondary organic aerosols.

In this study, we used GEOS-Chem version 13.2.1 in its high-performance implementation (GCHP). The flexibility and scalability of high resolution simulations in the standard offline version of GEOS-Chem (“GEOS-Chem Classic”) are limited,



as it relies on shared-memory parallelization and a rectilinear longitude-latitude grid (Martin et al., 2022). GCHP version 11, developed by Eastham et al. (2018), shares the same source code for physical and chemical mechanisms with GEOS-Chem Classic. It operates on a cubed-sphere grid with Message Passing Interface (MPI) distributed memory framework for massive parallelization by coupling the Model Analysis and Prediction Layer (MAPL) (Suarez et al., 2007) of the NASA GMAO with Earth System Modeling Framework (ESMF) (Hill et al., 2004). Together with the development of Finite-Volume Cubed-Sphere Dynamical Core (FV3) from Geophysical Fluid Dynamics Laboratory (GFDL) (Harris et al., 2016), GCHP version 13 could operate on a stretched cubed-sphere grid to enhance grid resolution in a customised region with smooth, gradual changes in resolution (Bindle et al., 2021).

2.2 Fire emission inventory

Fire emission inventories were developed to convert satellite detection of fires into numerical emission inputs for chemical transport models (CTMs) or Earth system models with atmospheric chemistry to simulate and analyze the emission patterns and impacts (Liu et al., 2020). In this study, we employed the Global Fire Emission Dataset version 4 (GFEDv4s), the built-in fire emission inventory in GCHP. GFEDv4s utilizes the Moderate Resolution Imaging Spectroradiometer (MODIS) Collection 5.1 MCD64A1 burned area product at 500-m spatial resolution to estimate the burned areas. It also incorporates 1-km thermal anomalies data from MODIS Terra and Aqua and 500-meter surface reflectance observations to account for the burned area of small fires in 0.25 degrees (BA_{sf}) (van der Werf et al., 2017). This treatment of small fires improves accuracy, making GFEDv4s one of the best inventories to capture the magnitudes of observed smoke $PM_{2.5}$ in a regional case study in Indonesia (Liu et al., 2020). Additionally, GFEDv4s introduces a new burned fraction equation to estimate subgrid burned fractions in frequently burned landscapes, which are commonly found in the southeastern part of the Amazon. This modified approach adjusts the fuel load in grid cells that burn in previous months and avoids the underestimation of emissions in frequently burning regions, especially toward the end of the fire season (van der Werf et al., 2017).

Moreover, GFEDv4s adjusts the fuel consumption rates based on the field measurement database developed by van Leeuwen et al. (2014) and Scholes et al. (2011). The detailed fuel consumption database is available from <https://www.geo.vu.nl/~gwerf/FC/>. The satellite-measured and ground-observed information is then provided to a biogeochemical model based on the Carnegie-Ames-Stanford Approach to generate the dry matter burned (DMB) data (van der Werf et al., 2017). By applying the new set of emission factors (in g species per kg dry matter burned), which are species-specific and fire type-specific, we are able to resolve trace gas and aerosol emissions from different fire types in Amazon for our study (van der Werf et al., 2017). The detailed emission factors are available in the supplementary material (Table S1).

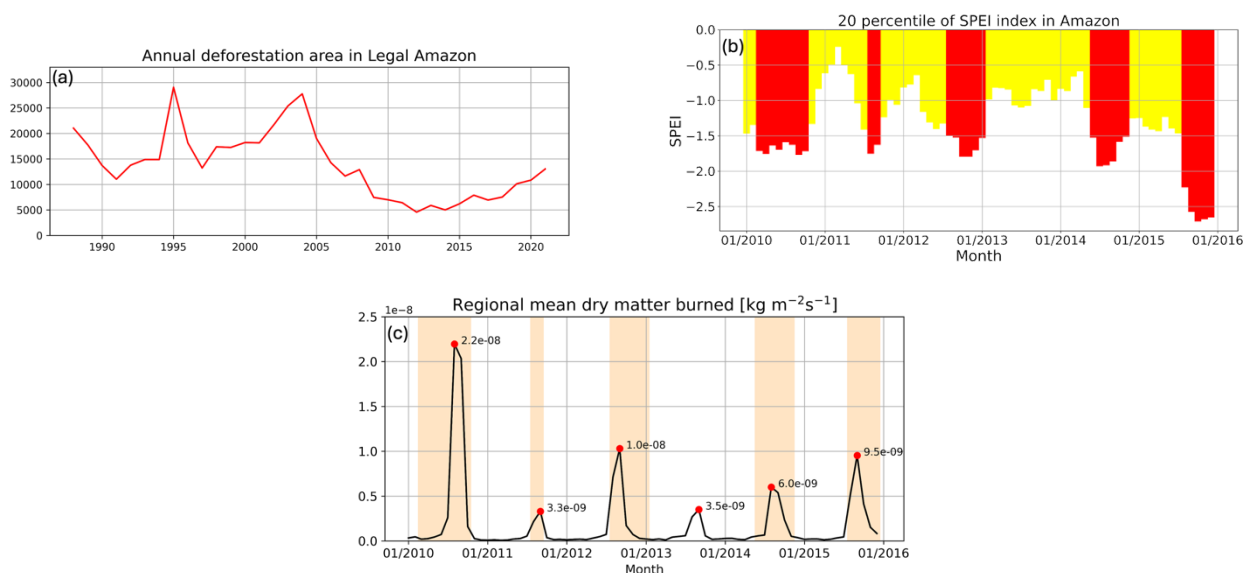
2.3 Deforestation and Drought data

Recent research on GFED time series data found that 55% of the smoke emission from 1997 to 2015 originated from deforestation fires (van Marle et al., 2017). The Amazon deforestation data used in this project were retrieved from



165 TerraBrasilis, which relies on Landsat and MODIS satellite data to monitor and analyze land cover changes in the Amazon
rainforest through The Amazon Deforestation Monitoring Project (PRODES) and The Real Time System for Detec-
tion of Deforestation (DETER) systems, developed by the Instituto Nacional de Pesquisas Espaciais (INPE) (F. G. Assis et al.,
2019; Prodes, 2013). The Brazilian government has implemented the Action Plan for Prevention and Control of Deforestation
in Amazonia (PPCDAm) in order to protect the Amazon rainforest from illegal deforestation and aim for sustainable
170 development since 2005 (Aragão et al., 2018). After three phases of PPCDAm, the annual deforestation rate was reduced to
one-third of the average deforestation rate between 1988 and 2004 during 2010 to 2015 (Fig. 1a), which was stable in
magnitudes ($\sim 7,000 \text{ km}^2$) and favorable to the study on drought-induced air quality impacts.

The standardised precipitation-evapotranspiration index (SPEI) is a widely used multiscalar (30, 90, 180, 360, 720 days) drought
175 index based on water balance combining precipitation and potential evapotranspiration derived from climate data (Beguería et
al., 2014; Vicente-Serrano et al., 2010). The positive (negative) values of SPEI indicate wet (dry) condition. In this study, we
used the 3-month SPEI index to monitor the agricultural drought conditions in the Amazon rainforest. Figure 1b shows the
time series of the 20th percentile of regional SPEI index. The indices less than or equal to -1.5 are labeled with red color bars,
indicating the occurrence of a severe drought, while yellow color bars refer to non-drought conditions with the index larger
180 than -1.5 . In this study, the severe dry months were considered as experiencing a drought if they were extended to more than
three months. Therefore, according to the SPEI index, drought events occurred in 2010, 2012, 2014 and 2015, with the longest
duration lasting for eight months in 2010 and the strongest SPEI signal exceeding -2.5 in 2015, indicating extreme drought
conditions during these years, which aligns with other literatures (Espinoza et al., 2024; Papastefanou et al., 2022).



185

Figure 1: (a) Annual deforestation rate in Amazon, (b) 20th percentile of SPEI (3-month) index in Amazon, where red indicates severe dry months with index less than -1.5 , and (c) time series plot of regional mean dry matter burned recorded GFED. Red dots are the annual peak, and the shaded area indicates severe dry months.



2.4 Model experimental design

190 Here we employed GCHP version 13.2.1, with stretch grid factor 4 targeted in 3° S, 60° W and 72 vertical levels in cubed-
sphere grid C48, which allowed us to resolve the spatial resolution in the Amazon rainforest to ~0.5° (~50 km). We adopted
data from The Modern-Era Retrospective analysis for Research and Application, Version 2 (MERRA-2) (Gelaro et al., 2017)
as the meteorological input (http://wiki.seas.harvard.edu/geos-chem/index.php/List_of_MERRA-2_met_fields). The
emissions in GCHP are handled by The Harvard-NASA Emission Component (HEMCO version 3.1.1) (Lin et al., 2021),
195 which integrates various data inventories and scale factors. We implemented The Community Emissions Data System, Version
2 (CEDSV2) (McDuffie et al., 2020) for global base anthropogenic emissions and The Model of Emissions of Gases and
Aerosols from Nature version (MEGAN) (Guenther et al., 2012) for biogenic emissions in all simulations.

Two sets of simulations ran from January 2009 to December 2015 to investigate the drought impacts where the first year served
200 as the model spin-up, and model results from 2010 to 2015 were analyzed. The deforestation rate remains low and stable during
the experimental period (Fig. 1a), enabling us to investigate the drought impacts by comparing the air quality between drought
years (2010, 2012, 2014 and 2015) and non-drought years (2011 and 2013). The first set of simulations (“fire-on”) utilized the
GFEDv4s (Randerson et al., 2018) monthly DMB data in 0.25° to represent fire emissions (Fig. 1c), while the second set of
simulations (“fire-off”) were the control without any biomass burning. The DMB recorded by GFEDv4s peaks in every August
205 or September while the magnitudes in drought years generally double to triple that in non-drought years, except the outliers in
2010 where its magnitude doubles to that in other drought years. By utilising the GFEDv4s data in GCHP, we obtained the
fire-induced chemical emissions by multiplying the species-specific and fire-type-specific emission factors (see Table S1 for
details) with DMB, and thus conducted a temporal analysis of shortlisted chemicals in monthly level from Jan 2010 to Dec
2015 within the Brazilian Amazon area (5°N-15°S, 47°W-73°W) and spatial analysis of the chemicals of concern in monthly
210 level from January 2009 to December 2015 in South America (15°N-25°S, 40°W-90°W).

2.5 Estimation of fire-induced premature mortality

We compared the simulated surface PM_{2.5} and ozone concentrations from the two sets of simulations (“fire-on” and “fire-off”) together with satellite-observed PM_{2.5} concentrations to quantify the fire-induced health impacts in terms of premature deaths. The PM_{2.5} concentrations in GCHP were calculated as the sum of ammonium, inorganic nitrates, sulfate, black carbon, organic
215 carbon, dust aerosol (first two size bins), fine sea salt aerosol (first size bins) and secondary organic aerosol (SOA). The full
definition and detail equations used in GCHP can be found on the GEOS-Chem wiki (http://wiki.seas.harvard.edu/geos-chem/index.php/Particulate_matter_in_GEOS-Chem).

To estimate the premature mortality due to exposure to fire-induced PM_{2.5}, we applied satellite-derived monthly PM_{2.5}
220 concentrations (V5.GL.04), provided by the Atmospheric Composition Analysis Group of the Washington University in St.



Louis (Shen et al., 2024) and a monthly grid-specific correction factor derived from the two sets of simulations for the counterfactual situation to the GEMM NCD+LRI model established by Burnett et al. (2018). The counterfactual PM_{2.5} concentration is given by:

$$PM_{2.5c} = \frac{\text{GCHP fire off } PM_{2.5}}{\text{GCHP fire on } PM_{2.5}} \times \text{satellite } PM_{2.5}, \quad (1)$$

225 The GEMM NCD+LRI model estimates PM_{2.5}-induced premature deaths using age-specific and sex-specific hazard ratios, baseline mortality and population data. The hazard ratio (HR) is given by:

$$HR(z) = \exp \left\{ \frac{\theta \log \left(\frac{z+1}{\alpha} \right)}{1 + \exp \left(-\frac{z-u}{v} \right)} \right\}, \quad (2)$$

where

$$z = \max (0, PM_{2.5} - 2.4 \mu\text{g m}^{-3}), \quad (3)$$

230 and θ , α , u , v are disease-specific and age-specific parameters describing the shape of hazard ratio function with 2.4 $\mu\text{g m}^{-3}$ as the counterfactual PM_{2.5} concentration described by Burnett et al. (2018). The number of PM_{2.5}-induced premature death (M) is given by:

$$M = \frac{HR-1}{HR} \times B \times P \times A, \quad (4)$$

where B is the baseline mortality rate, P is the age-specific and sex-specific population, A is the grid area in each grid cell.

235 Baseline mortality rates are a disease-specific parameters for 12 age groups (25-29, 30-34, 35-39, 40-44, 45-49, 50-54, 55-59, 60-64, 65-69, 70-74, 75-79, 80 or above) and two sex groups (male and female), obtained from Global Burden of Disease (GBD) (<https://vizhub.healthdata.org/gbd-results/>). Detailed information can be found in supplementary material (Table S2). Population data for each age groups and sex groups were derived from the 2010 population density estimated by Gridded Population of the World, version 4, revision 11 (GPWv4.11) (Center for International Earth Science Information Network, 240 2018). The aggregated population density is detailed in supplementary material (Fig. S1). This dataset was produced as global rasters at 30 arc-second horizontal resolution and aggregated to 2.5 arc-minute, about 4.6 km at the equator. We regridded this population dataset to match our simulation output from GCHP for further analysis.

To estimate premature deaths induced by ozone exposure, we utilize established exposure-response relation from previous 245 studies (Anenberg et al., 2010; Malley et al., 2017; Seltzer et al., 2018).

$$HR = \exp^{\beta \Delta Y}, \quad (5)$$

$$AF = 1 - \exp^{-\beta \Delta X}, \quad (6)$$

$$M = AF \times B \times P \times A, \quad (7)$$

where

$$250 \Delta X = \max (0, [O_3] - \text{counterfactual concentration}), \quad (8)$$

and HR is the hazard ratio reported by previous epidemiological study, ΔY is 10 ppb from epidemiological studies conducted by Jerrett et al. (2009) and Turner et al. (2016), AF is the attributable fraction of ozone exposure, ΔX is the simulated ozone



255 exposure with counterfactual concentration, β is the exposure-response factor, M is the number of ozone-induced premature deaths, B is the baseline mortality rate and P is the age-specific and sex-specific population, and A is the grid area in each grid cell. The baseline mortality and population data used here are consistent with those employed for estimating premature deaths caused by $PM_{2.5}$ exposure.

260 In this study, we used the averaging metric and cause-specific risks recorded by Jerrett et al. (2009) and Turner et al. (2016). Jerrett et al. (2009) used the April-September average of daily 1-hour maximum ozone concentration (6mMDA1) with counterfactual concentration 33.3 ppb, while Turner et al. (2016) focused on the annual average daily maximum 8-hour ozone concentration (AMDA8) with counterfactual concentration 26.7 ppb. For respiratory diseases, the hazard ratios of 1.040 (95% CI: 1.013, 1.067) from Jerrett et al. (2009) and 1.12 (95% CI: 1.08, 1.16) from Turner et al. (2016). In addition, we applied hazard ratio of 1.03 (95% CI: 1.01, 1.05) for cardiovascular mortality, also reported by Turner et al. (2016).

3 Results

265 3.1 GCHP model evaluation

We evaluated the ozone concentration against ground measurements over the Amazon region. The ground measurements of ozone were obtained from the Tropospheric Ozone Assessment Report (TOAR) (Gaudel et al., 2018). In the first phase of TOAR, there are five ground stations in the Brazilian Amazon monitoring surface ozone concentration. “Br-am01”, “br-am04” and “br-am05” are located near Manaus. “Br-am02” is located near Santarém. “Br-am03” is near Porto Velho. These station locations are available in the supplementary material (Table S3). These measured ozone concentrations are compared with the GCHP-simulated results in the bottom layer of the nearest grid cell (Fig. S2). Among the five stations, the best estimation is station “br-am02”, in which the ozone level from Sep 2014 to Sep 2015 is highly similar to the measured concentration. Additionally, GCHP is able to reproduce the similar ozone level in station “br-am01” during late 2010 but slightly overestimate the ozone level during 2014. For the other three stations, the model successfully reproduce the temporal pattern but overestimate ozone levels. As these five TOAR stations are at different altitudes, ranging from 25 m to 261 m, the altitude difference between the measurement sites and GCHP simulation grid cells may cause such overestimation. Moreover, the performance discrepancies may also be caused by the low plume height of tropical forest fires and savanna fires as suggested by Gonzalez-Alonso et al. (2019), especially under drought conditions. With an updated emission injection scheme, GEOS-Chem can better simulate the vertical distribution of peroxyacetyl nitrate (PAN) and CO to match the observations in summer (Zhu et al., 2018) and consequently better estimate ozone concentrations.

We also validated the simulated surface $PM_{2.5}$ concentrations by comparing them with satellite-derived surface $PM_{2.5}$, which is from a global monthly mean dataset with 1° spatial resolution (named as V5.GL.04), provided by the Atmospheric Composition Analysis Group of the Washington University in St. Louis (Shen et al., 2024). We compared the performance



285 between dry (Jul-Nov) and wet (Jan-May) season for every year, including both drought and non-drought years (Fig. S3).
Despite the overall underestimation of PM_{2.5} concentrations, there are significant seasonal variations because the contribution
from wildfire emissions to regional PM_{2.5} concentration is much higher during the dry season. GCHP with GFEDv4s fire
emission inventory has a better performance in the dry season and overall underestimate surface PM_{2.5} when compared to
satellite data, especially in non-drought years (2011 and 2013). Among all drought years, the model performs better in years
290 with severe drought, with $R^2 = 0.55$ in 2010 and $R^2 = 0.42$ in 2015. The high concentrations are likely dominated by fire
emissions during the dry season with severe droughts, and therefore reduce the discrepancies from other emissions. Figure S4
illustrates the time series comparison between the simulated surface PM_{2.5} from GCHP with GFEDv4s and the satellite-derived
surface PM_{2.5} obtained from V5.GL.04 between Jan 2010 to Dec 2015. Although underestimation is noticeable in the temporal
patterns, they show a strong correlation, mirroring the trends as in the satellite-derived data. This indicates that, despite the
295 general underestimation, the model captures the seasonal dynamics of PM_{2.5} variation and aligns well with satellite
observations.

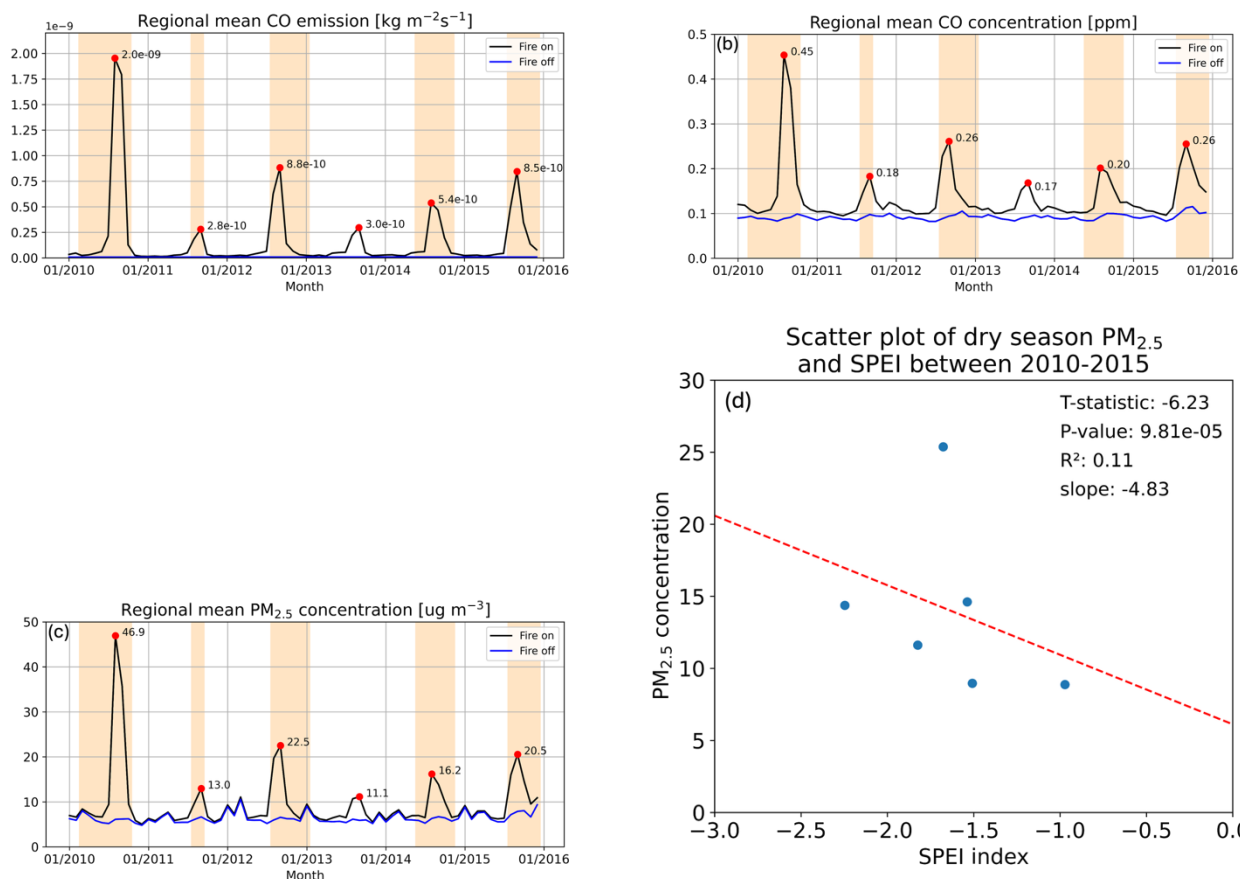
To investigate the underlying sources of biases between simulated PM_{2.5} concentrations and satellite observations, we apply a
machine learning algorithm, specifically the Light-GBM model. By treating these biases as the predicted variable, we can
300 systematically analyze how various factors contribute to the discrepancies observed. In this model, we utilized several key
predictors, including ERA5 meteorological variables, such as surface temperature, wind speed, and humidity, to gether with
detailed emission inventories, such as GFED and CEDS, that provide information on pollution sources (Fig. S5). The Light-
GBM model revealed that surface wind speed is the strongest predictor, indicating its significant influence on the observed
bias. Relative humidity and surface temperature are the other two important variables, suggesting meteorological condition is
305 the main cause of the model-observation bias. Therefore, we applied satellite-derived monthly PM_{2.5} concentrations
(V5.GL.04) and a monthly grid-specific correction factor generated from the simulations to get better estimation for the health
impact analysis.

3.2 Carbon monoxide (CO) and fine particulate matter (PM_{2.5})

310 CO is harmful because of its ability to displace oxygen in human blood cells and thus reduce blood oxygen levels (Byard,
2019). Figure 2a shows its emissions in the Amazon, which are highly dependent on the incomplete combustion from
deforestation fires. Therefore, CO emissions in the fire-off simulations remain at low levels (9×10^{-12} kg m⁻² s⁻¹), while the
emission pattern in fire-on simulation was highly similar to the pattern of DMB shown in Fig. 1. The annual CO emission
peaks were either in August or September because of the high fire occurrences during the dry season. The annual emission
315 peaks in drought years (5.4 to 8.8×10^{-10} kg m⁻² s⁻¹) are generally two to three times higher than those in non-drought years
(2.8 to 3.0×10^{-10} kg m⁻² s⁻¹), while the emission in 2010 is also an outlier, reaching 2.0×10^{-9} kg m⁻² s⁻¹ as the annual peak.
Figure 2b shows the fire-on and fire-off monthly mean CO concentration from 2010 to 2015. The concentration in the fire-off



simulation remains low and stable at level of 0.095 ppm while the concentration in fire-on simulation fluctuates and also peaks in every August and September, identical to the emission pattern. Due to the higher emission rate in dry season with drought events, the annual peak of the Amazon monthly mean CO concentration in 2010, 2012, 2014 and 2015 is consequently higher than that in 2011 and 2013. The average magnitude of annual peak during drought years is 0.29 ppm and that during non-drought years is just 0.18 ppm. Therefore, by comparing it to the concentration in fire-off simulation (0.095 ppm), fire emission contributes to about 50% of the annual peak CO concentration in non-drought years and such proportion would further increase to about 67% in drought years. Figure 3a shows the dry season mean CO concentration from 2010 to 2015 from the fire-on simulation. These spatial concentration plots show that the high CO concentration pattern is mostly localized, suggesting that the concentration is associated with fire occurrence, which agrees with our finding from the time series plots.



330 **Figure 2: Simulated monthly mean carbon monoxide (CO) (a) emission, (b) concentrations and (c) PM_{2.5} concentrations from Jan 2010 to Dec 2015 in Brazilian Amazon. Red dots are the annual peak and the shaded area indicated dry months where 20th percentile of regional SPEI index smaller than -1.5. (d) Scatter plot of dry season regional mean PM_{2.5} and the dry season mean SPEI index.**

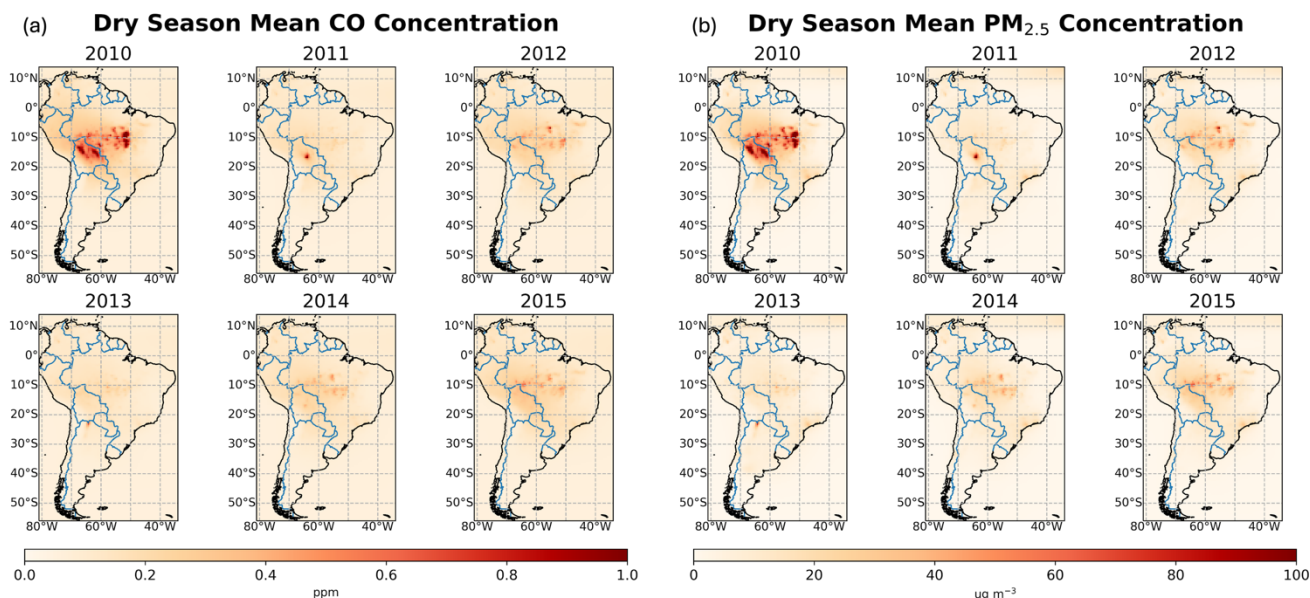


Figure 3: Dry season mean carbon monoxide (CO) and particulate matter (PM_{2.5}) concentration simulation between 2010 and 2015.

335

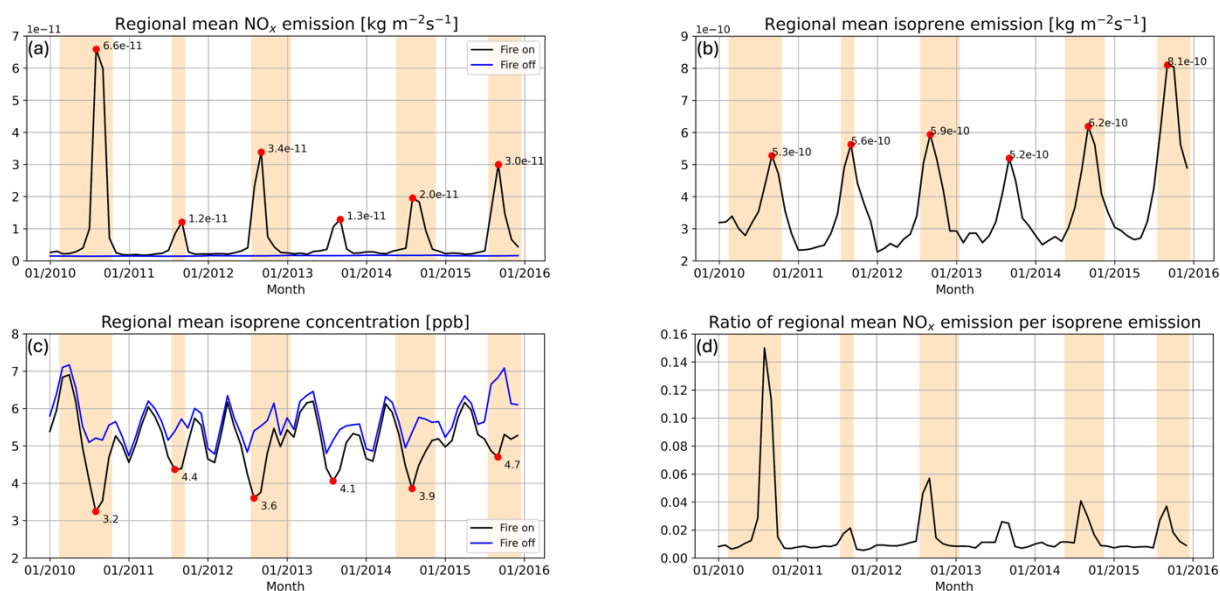
Figure 2c shows the simulated Amazonian monthly mean PM_{2.5} concentration in fire-on and fire-off simulations from 2010 to 2015. PM_{2.5} concentration is similar to the CO concentration pattern because both of them are the primary pollutants generated by incomplete combustion during deforestation and savanna fires. The PM_{2.5} concentration in the fire-off simulation is stable and stays between 6 to 10 $\mu\text{g m}^{-3}$ throughout the study period while the concentrations in the fire-on simulation are higher during dry seasons in both non-drought and drought years. The annual peak of PM_{2.5} concentration in non-drought years is around 12 $\mu\text{g m}^{-3}$, while the average annual peak in drought years is 26 $\mu\text{g m}^{-3}$ with an extreme high record reaching 46.4 $\mu\text{g m}^{-3}$ in 2010. The fire-induced PM_{2.5} accounts for about 50% of the regional concentration during the dry season in non-drought years, and enhances the dry season concentration in drought years to a level of two to four times higher than that in non-drought years. To further understand the relationship between droughts and PM_{2.5}, we compared between the dry season mean PM_{2.5} concentration and SPEI drought index (Fig. 2d). As the negative value of SPEI indicates drought occurrence, the negative slope (-4.83) in linear regression suggests that PM_{2.5} concentration increases with the intensity of drought. The t -value and p -value are -6.23 and 9.81×10^{-5} respectively with an outlier in 2010, suggesting we can reject the null hypothesis of no difference under drought and non-drought conditions. Therefore, fire emissions lead to regional PM_{2.5} sources and droughts worsen the pollution by influencing fires in the Amazon forest. Figure 3b shows the dry season mean PM_{2.5} concentration from 2010 to 2015 from the fire-on simulation. Similar to the CO spatial pattern, the PM_{2.5} concentration pattern is mostly localized and rapidly diluted, suggesting PM_{2.5} concentration is associated with fire emission with a short lifetime in the surface layer.

350



3.3 Nitrogen oxide (NO_x) and ozone (O₃)

NO_x is a group of highly-reactive gases including nitric oxide (NO) and nitrogen dioxide (NO₂), emitted from both anthropogenic sources (such as industrial combustion and transportation) and natural sources (such as lightning and wildfires). NO_x, together with volatile organic compounds (VOCs) and solar radiation, is the precursor of tropospheric ozone. Figure 4a shows the Brazilian Amazon monthly mean NO_x emission in both simulations. Similar to CO and PM_{2.5}, NO_x emission in the fire-off simulation remains low and stable with $5.0 \times 10^{-12} \text{ kg m}^{-2} \text{ s}^{-1}$ throughout the simulation period, while NO_x emission in the fire-on simulation increases with similar pattern as enhanced DMB, indicating that NO_x emissions in Brazilian Amazon are also dominated by wildfires. In the meantime, drought events amplify the NO_x emission to two to four times (2.0 to $3.4 \times 10^{-11} \text{ kg m}^{-2} \text{ s}^{-1}$) higher than that during non-drought years (1.2 to $1.3 \times 10^{-11} \text{ kg m}^{-2} \text{ s}^{-1}$), in which 2010 is the outlier with the annual peak emission rate up to $6.6 \times 10^{-11} \text{ kg m}^{-2} \text{ s}^{-1}$. Figure 4b shows the simulated isoprene, one of the major biogenic VOC (BVOC), emissions in Brazilian Amazon, which is simulated by MEGAN independent of the impacts of wildfires. Therefore, isoprene emission remains the same in both sets of simulations and peaks in every September with a magnitude from 5.2 to $8.1 \times 10^{-10} \text{ kg m}^{-2} \text{ s}^{-1}$. Even though the annual emission peak is in September, the annual minimum of monthly mean isoprene concentration in fire-on simulation is also found between August and September. The annual minimum of monthly mean isoprene concentration in the fire-on simulation (3.2 to 4.7 ppb) is 1 to 2 ppb lower than that in fire-off simulation in the same period of time (Fig. 4c). We also estimate the ratio of NO_x emission over isoprene emission in Fig. 4d. The ratio remains in a low proportion (below 0.16), suggesting that NO_x is the limiting factor of surface ozone formation in the Amazon and fire emissions are the primary factor to generate NO_x and ozone to worsen the regional air quality.

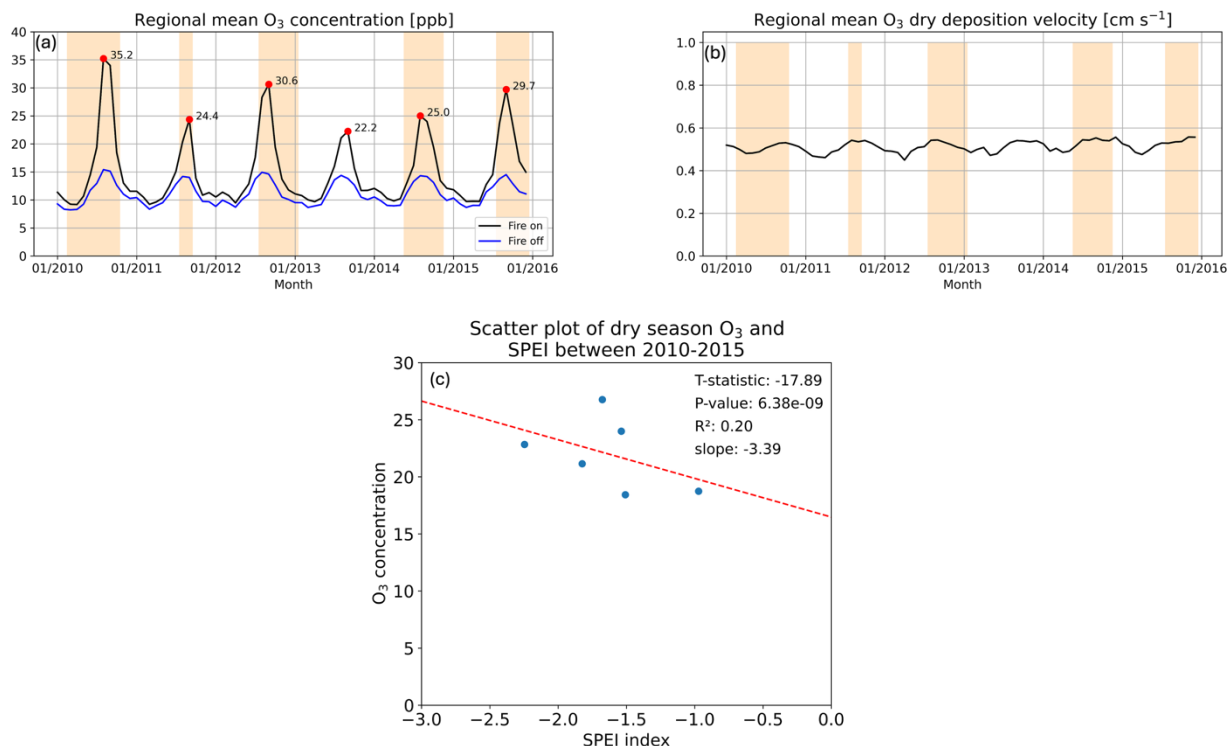


375 **Figure 4: Simulated monthly mean (a) nitrogen oxide (NO_x) emission, (b) isoprene emission and (c) isoprene concentration from Jan 2010 to Dec 2015 in Brazilian Amazon. (d) Time series of NO_x and isoprene emission ratio from 2010 to 2015. Red dots are the annual peak (low) and shaded area indicated dry months where 20th percentile of regional SPEI index smaller than -1.5 .**



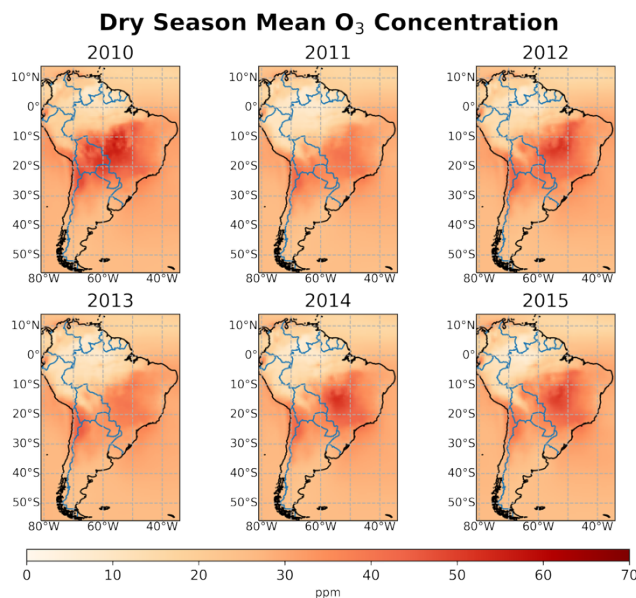
Figure 5a shows the simulated Amazon monthly mean ozone concentration in fire-on and fire-off simulations from 2010 to 2015. There is an annual concentration peak in every August in both fire-on and fire-off simulations. However, the annual ozone concentration peak is about 14 ppb in the fire-off simulation, while it ranges from 22.1 to 24.2 ppb during non-drought years and 24.9 to 35.1 ppb during drought years in fire-on simulation. The fire-induced ozone concentration contributes to about one-third of the total concentration in non-drought years while the contribution ranged from one-third to more than 50% in drought years. To better demonstrate the impacts of droughts on ozone, we compare dry season mean ozone concentration and SPEI drought index (Fig. 5c). As the negative value of the SPEI indicates drought occurrence, the negative slope (-3.39) in linear regression suggests that ozone concentration increases with the intensity of drought. The t -value and p -value are -17.89 and 6.38×10^{-9} respectively, suggesting we can reject the null hypothesis of no difference between drought and non-drought conditions.

Despite the lower contribution fraction-wise of fires to ozone concentration than for CO and PM_{2.5}, ozone pollution induced by fire emission is a regional air quality issue. Figure 5b shows the dry deposition velocity of ozone in the Amazon, which is mainly determined by meteorological and land use conditions. With stable dry deposition velocity throughout the simulation period, ozone dry deposition rates mainly depend on its concentration, leading to higher deposition rates in drought years than non-drought years and consequently causing more damage to the vegetation and ecosystems in drought years. Figure 6 shows the fire emission contribution of dry season mean ozone concentration from 2010 to 2015, generated by grid-to-grid comparison of the two simulations. These spatial concentration plots show that the fire-emitted ozone was advected toward the southern part of the Brazil, suggesting the affected area of ozone is larger than that of PM_{2.5} and causing regional air pollution. Moreover, the fire emission contribution of ozone concentration shows a larger impact area during dry season in drought years than during non-drought years. Therefore, fire emission is suggested to be one of the dominant sources deteriorating regional ozone pollution, and drought events would further worsen it in both pollutant magnitude and impact area by amplifying fire emissions in Amazon forest.



400

Figure 5: (a) Simulated monthly mean ozone concentration and (b) dry deposition from Jan 2010 to Dec 2015 in Brazilian Amazon. Shaded area indicated dry months where 20th percentile of regional SPEI index smaller than -1.5. (c) Scatter plot of dry season regional mean ozone and the dry season mean SPEI index.



405 Figure 6: Dry season mean ozone concentration simulation between 2010 and 2015.



3.4 Impacts on public health

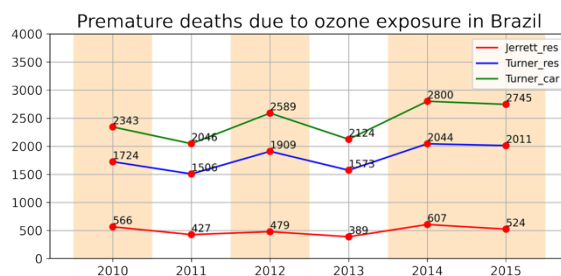
Utilizing the GEMM NCD+LRI model with GCHP simulated grid-specific correction on satellite-derived monthly mean PM_{2.5} concentrations, population density, and cause-specific baseline mortality rates, we also estimated the premature deaths induced by PM_{2.5} exposure in Brazil from 2010 to 2015. The total PM_{2.5}-induced premature deaths showed a fluctuating trend over the simulated period (Fig. 8). The PM_{2.5} induced death is estimated to be 22,595 in 2010 and 22,931 in 2011. There is a slight decrease to 21,621 in 2012, 22,081 in 2013 and 22,068 in 2014 but then shows substantial increase to 23,113 in 2015. The total ozone induced premature mortality is comparably lower than that of PM_{2.5}, causing 4,227 deaths in 2010, 3,693 in 2011, 4,676 in 2012, 3,844 in 2013, 4,104 in 2014 and 4,943 in 2015 (Fig. 9a).

415

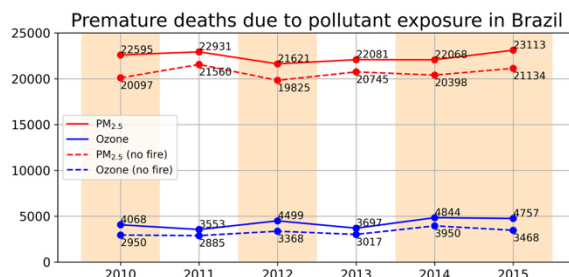
Utilizing averaging metrics and exposure-response relationships from Jerrett et al. (2009) and Turner et al. (2016), we estimated the annual premature mortalities induced by ozone exposure in Brazil with population density and cause-specific baseline mortality rates between 2010 and 2015. Using the methods of Jerrett et al. (2009), the premature mortalities due to respiratory diseases caused by exposure to ozone in Brazil from 2010 to 2015 are 566 (95% CI: 146-832), 427 (95% CI: 110-630), 479 (95% CI: 123-707), 389 (95% CI: 100-574), 607 (95% CI: 157-892) and 524 (95% CI: 135-772) (Fig. 7). When using Turner et al. (2016)'s exposure-response relationship, the estimated premature mortalities due to respiratory diseases caused by ozone exposure are higher, which are 1,724 (95% CI: 1,242-2,254), 1,506 (95% CI: 1,061-1,970), 1,909 (95% CI: 1,344-2,497), 1,573 (95% CI: 1,106-2,061), 2,044 (95% CI: 1,444-2,664), and 2,011 (95% CI: 1,420-2,623) from 2010 to 2015 (Fig. 10). Apart from respiratory diseases, Turner et al. (2016) included cardiovascular diseases into premature mortalities estimations, which are 2,343 (95% CI: 798-3,827) in 2010, 2,046 (95% CI: 696-3,343) in 2011, 2,589 (95% CI: 881-4,231) in 2012, 2,124 (95% CI: 722-3,474) in 2013, 2,800 (95% CI: 955-4,566) in 2014, and 2,745 (95% CI: 936-4,479) in 2015 (Fig. 8).

In the following discussion, Turner's exposure-response relationship will be prioritized, as it includes both cardiovascular and respiratory diseases, offering a more comprehensive assessment of health impacts compared to Jerrett's model, which focuses solely on respiratory diseases. Additionally, Turner's model, established in 2016, provides more up-to-date and relevant data compared to Jerrett's 2009 study, making it a more robust choice for this analysis.

430

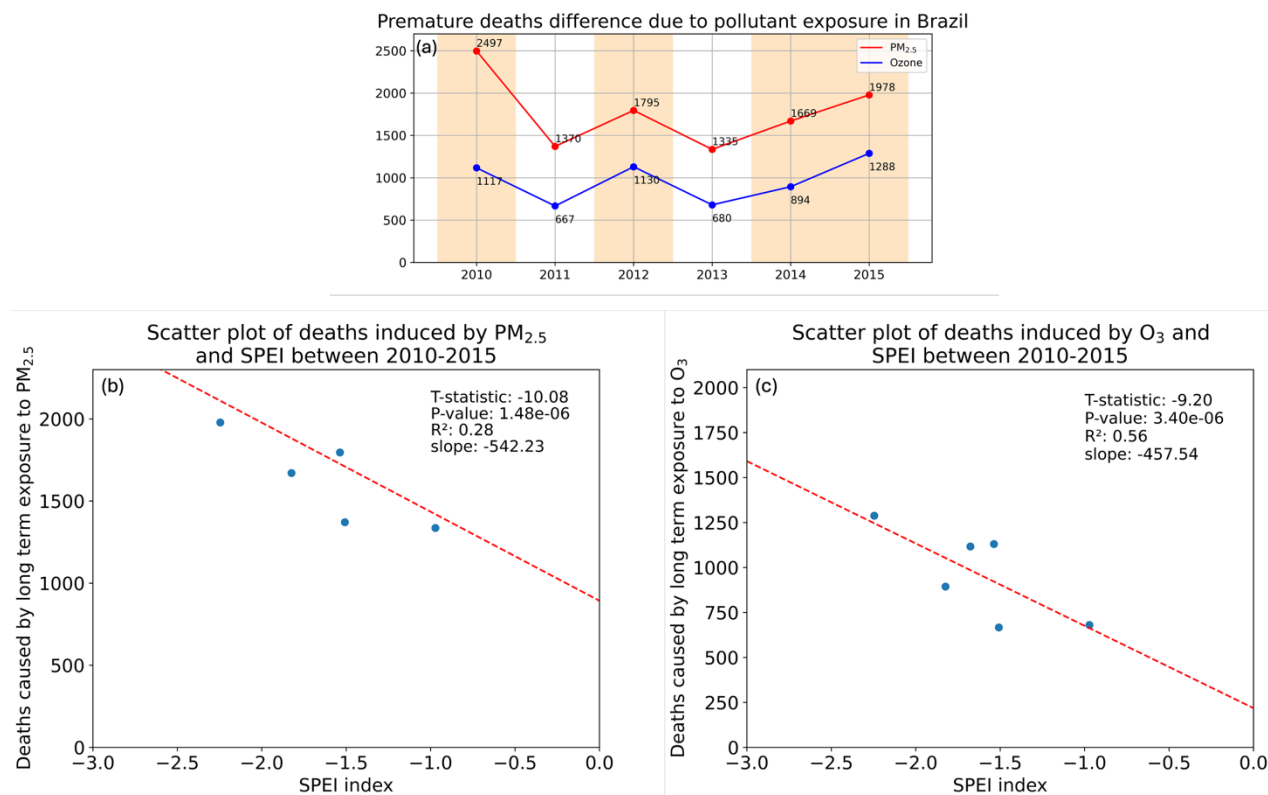


435 **Figure 7: Timeseries of annual premature mortalities due to exposure to ozone using exposure-response relation from Jerrett et al. (2009) (red) and Turner et al. (2016) (blue: respiratory diseases; green: cardiovascular diseases). Shaded area indicated years with more than three months which 20th percentile of regional SPEI index smaller than -1.5 .**



440 **Figure 8: Timeseries of annual excess mortalities due to exposure to PM_{2.5} (red) and ozone (blue) in “fire-on” (solid line) and “fire-off” (dotted line) simulations. Shaded area indicated years with more than 3 months which 20th percentile of regional SPEI index smaller than -1.5 .**

Although there is not an obvious trend in the total number of premature deaths, the difference in PM_{2.5}- and ozone-induced premature deaths between fire-on and fire-off simulations align closely with the drought index (SPEI). Figure 9a shows that the fire-induced premature mortalities due to exposure to PM_{2.5} and ozone were significantly higher in drought years than in non-drought years. By comparing the estimated premature deaths with control simulations, we found that fire-induced PM_{2.5} and ozone cause 6.0% and 18.6% more deaths in non-drought years, and 8.9% and 24.4% more in drought years. Such differences in terms of premature mortalities are obviously larger in years with strong drought events (2010 and 2015). Figure 9b and 9c also demonstrates the correlation between the SPEI drought index and fire-induced premature mortalities due to exposure to PM_{2.5} and ozone. As the negative value of SPEI indicates drought occurrence, the negative slopes in linear regression from both graphs suggest that the number of deaths caused by PM_{2.5} and ozone both increases with drought intensity. For PM_{2.5}, the *t*-value and *p*-value are -10.08 and 1.48×10^{-6} . For ozone, the *t*-value and *p*-value are -9.20 and 3.4×10^{-6} . Such statistics suggest that both null hypotheses can be rejected and that there are significant statistical differences of fire-induced premature mortalities between drought years and non-drought years.



460 **Figure 9: (a) Fire-induced premature mortalities due to exposure to PM_{2.5} (red) and ozone (blue). Shaded area indicated years with more than 3 months which 20th percentile of regional SPEI index smaller than -1.5. Scatter plots between SPEI drought index and fire-induced premature mortalities due to exposure to (b) PM_{2.5} and (c) ozone.**

465 Furthermore, despite premature deaths induced by exposure to ozone being lower than that to PM_{2.5}, the health impact induced by ozone is more sensitive and closely correlated to drought conditions with an $R^2 = 0.56$. The major reason behind is the difference in lifetime between these two pollutants. Ozone and its precursors could be advected to highly populated areas with longer lifetimes, while PM_{2.5}-induced impacts were mostly localized within more scarcely populated areas.

4 Discussion and conclusions

470 In this study, we utilized the fire emission inventory GFEDv4s in the GCHP global chemical transport model to perform “fire-on” and “fire-off” simulations and then compared simulated pollutant concentrations to study the fire-induced impacts between 2010 and 2015 in Brazil. We also investigated the interannual variability of dry season pollutant concentrations in the Brazilian Amazon by analyzing the simulation results with deforestation data and SPEI index. We demonstrated that biomass burning emissions are the dominant factor shaping air quality in Brazilian Amazon during the dry season. The proportion of pollutant concentrations contributed by biomass burning is even higher during drought events than that in non-drought years between



2010 and 2015, where the annual deforestation rate is stable at rate around 5,500 km². We found that droughts worsen air
475 quality through enhanced fire emissions, but different pollutants increase to various extents. For primary pollutants (CO and
PM_{2.5}), the fire contribution to dry season regional averaged concentration was about 50% during non-drought years and up to
60–80% during drought years. For secondary pollutant (ozone), the fire contribution to dry season regional averaged
concentration is about 33% during non-drought years and up to 50% during drought years. Statistically significant correlations
between pollutant (PM_{2.5} and ozone) concentrations and drought intensity were also found. We also quantified the health
480 impacts of fire-induced pollutants in terms of premature deaths under different climate conditions. The fire-induced PM_{2.5} and
ozone caused 6.0% and 18.6% more deaths in non-drought years, 8.9% and 24.4% more in drought years.

Our findings are broadly consistent with those of the few studies on biomass burning and interannual variability of fire
emissions in the Amazon. For instance, Mataveli et al. (2021) suggested that deforestation is important but not the only driver
485 of the emissions in the Amazon. de Moura et al. (2024) demonstrated that wildfires had an important influence on PM_{2.5} and
ozone levels with significant differences between days with fires and without fires. The drought impacts on fire emissions with
low deforestation rate we found were also found in the remote sensing and statistical study of Aragão et al. (2018), which
suggested that major droughts are caused by rainfall shortage influenced by sea surface temperature anomalies in Atlantic and
Pacific. Our results comparing the emission pattern between two major droughts (2010 and 2015) are also consistent with the
490 anomaly analysis on remote sensing data conducted by Silva Junior et al. (2019), which also found that drought-induced fire-
emitted CO₂ in 2010 dry season is higher than that in 2015 dry season.

Our findings further highlight the long-distance transport of fire-induced pollutants and their corresponding health impacts.
Despite most of the fires originating and concentrated in southern Amazon, we found that these fire-induced pollutants are
495 able to advect toward the highly populated regions in Brazil and even southern part of South America. Similar fire-induced
health impacts were also mentioned in previous studies. Butt et al. (2021) used the Weather Research and Forecasting Online-
Coupled Chemistry Model (WRF-Chem) with GEMM NCD+LRI and found that about 3,400 additional human deaths are
related to the increase in fire count in 2019. Bonilla et al. (2023) applied a linear concentration-response function (CRF) from
Vodonos et al. (2018) on GEOS-Chem simulations and found that about 12,000 deaths per year are induced by exposure to
500 smoke PM_{2.5} from 2014 to 2019 in South America. Such excess premature deaths are similar to our estimation and the
differences are related to the selection of CRF. Burnett et al. (2018) demonstrated that GEMM's hazard ratios exceed those
from integrated exposure-response model by 30–50% at low PM_{2.5} concentrations, suggesting GEMM prioritizes newer cohort
data at lower exposure levels. Moreover, Cobelo et al. (2023) suggested that wildfire impacts on air quality and health in Brazil
vary across land uses; in specific agricultural areas for soybean in the Amazon, it causes 3872 excess deaths.

505

Our simulations used a chemical transport model driven by historical meteorological, fire and land cover data that did not
account for the interactions and feedback between droughts, atmosphere and biosphere. For instance, the impacts of droughts



on plant phenology and atmospheric deposition processes might either amplify or suppress biogenic emissions. Besides, the fire emission data in our study, while scaled from the DMB recorded by the comprehensive global fire emission inventory
510 GFEDv4s with species-specific and fire type-specific emission factors, may contain uncertainties and inaccuracies in regional application (Liu et al., 2020). Previous studies found that the combination of net land use flux estimated from the Bookkeeping of Land Use Emissions (BLUE) and the net wildfire flux from a fire bookkeeping model (FATE) show similar interannual variability as GFEDv4s but the average flux from BLUE+FATE is 116% higher than GFEDv4s (Rosan et al., 2024). Future studies can incorporate the global fire emission inventory with a regional monitoring system, such as TerraBrasilis, to improve
515 representation on natural and deforestation fires (F. G. Assis et al., 2019), and couple the drought impacts on biosphere processes into coupled climate-chemistry models to further investigate the potential impacts of sea surface temperature anomalies on drought occurrence, fire emission and air quality.

Although the broader aspects are not covered in this study, this research confirms the significance of drought impacts on
520 regional air quality and health through influencing Amazon fire activities. As droughts intensify due to climate change and land use alterations, we expect a corresponding rise in PM_{2.5} and ozone levels, posing further health risks. Notably, the recent drought in 2023 underscores this concern, as prolonged dry conditions have led to an increase in fire activity, further deteriorating air quality (Espinoza et al., 2024; Miranda et al., 2026). The implications of our results extend beyond environmental concerns, as they can influence public health policies, air quality management, and agricultural practices.
525 Understanding the interactions between droughts and air quality is crucial for advancing several SDGs. Our results indicate that elevated PM_{2.5} and ozone levels enhance the health risks associated with respiratory and cardiovascular diseases, which is closely related to SDG 3 (Good Health and Well-being). Additionally, this research supports SDG 13 (Climate Action) by emphasizing the necessity for adaptive strategies in response to more frequent weather extremes (e.g., droughts). Implementing effective land use planning and resource management can alleviate the negative impacts of droughts on air quality, thus
530 promoting sustainable practices that enhance community health and resilience. By incorporating these findings into urban planning and development strategies, stakeholders can create healthier living environments that are more resilient to climate change effects. Ultimately, this study serves as a call to action for policymakers, researchers, and communities to collaborate on strategies that foster sustainable development while addressing the interconnected challenges of climate change, air quality, and public health.

535

Data availability. Model output data used for analysis and plotting can be made available in .nc format by contacting the corresponding author (Amos P. K. Tai at amostai@cuhk.edu.hk).



Author contributions. APKT and SS designed the study and supervised the writing of the paper. LTHN conducted model simulation, analyzed results, and wrote the draft with the assistance of JM, XL, SZ, FD and AL. All authors contributed to the discussion and improvement of the paper.

Competing interests. At least one of the (co-)authors is a member of the editorial board of Atmospheric Chemistry and Physics.

Acknowledgements. This work was supported by the CUHK-University of Exeter Joint Centre for Environmental Sustainability and Resilience (ENSURE; project no.: 4930820) awarded to A. P. K. Tai and S. Sitch.

References

- Albert, J. S., Carnaval, A. C., Flantua, S. G., Lohmann, L. G., Ribas, C. C., Riff, D., Carrillo, J. D., Fan, Y., Figueiredo, J. J., & Guayasamin, J. M. (2023). Human impacts outpace natural processes in the Amazon. *science*, 379(6630), eabo5003.
- Anenberg, S. C., Horowitz, L. W., Tong, D. Q., & West, J. J. (2010). An estimate of the global burden of anthropogenic ozone and fine particulate matter on premature human mortality using atmospheric modeling. *Environmental Health Perspectives*, 118(9), 1189-1195.
- Aragão, L. E. O. C., Anderson, L. O., Fonseca, M. G., Rosan, T. M., Vedovato, L. B., Wagner, F. H., Silva, C. V. J., Silva Junior, C. H. L., Arai, E., Aguiar, A. P., Barlow, J., Berenguer, E., Deeter, M. N., Domingues, L. G., Gatti, L., Gloor, M., Malhi, Y., Marengo, J. A., Miller, J. B., Phillips, O. L., & Saatchi, S. (2018). 21st Century drought-related fires counteract the decline of Amazon deforestation carbon emissions. *Nature Communications*, 9(1), 536. <https://doi.org/10.1038/s41467-017-02771-y>
- Aragão, L. E. O. C., Malhi, Y., Roman-Cuesta, R. M., Saatchi, S., Anderson, L. O., & Shimabukuro, Y. E. (2007). Spatial patterns and fire response of recent Amazonian droughts. *Geophysical Research Letters*, 34(7). <https://doi.org/https://doi.org/10.1029/2006GL028946>
- Aragão, L. E. O. C., Poulter, B., Barlow, J. B., Anderson, L. O., Malhi, Y., Saatchi, S., Phillips, O. L., & Gloor, E. (2014). Environmental change and the carbon balance of Amazonian forests. *Biological Reviews*, 89(4), 913-931. <https://doi.org/https://doi.org/10.1111/brv.12088>
- Beguéría, S., Vicente-Serrano, S. M., Reig, F., & Latorre, B. (2014). Standardized precipitation evapotranspiration index (SPEI) revisited: parameter fitting, evapotranspiration models, tools, datasets and drought monitoring. *International Journal of Climatology*, 34(10), 3001-3023. <https://doi.org/https://doi.org/10.1002/joc.3887>
- Bey, I., Jacob, D. J., Yantosca, R. M., Logan, J. A., Field, B. D., Fiore, A. M., Li, Q., Liu, H. Y., Mickley, L. J., & Schultz, M. G. (2001). Global modeling of tropospheric chemistry with assimilated meteorology: Model description and evaluation. *Journal of Geophysical Research: Atmospheres*, 106(D19), 23073-23095. <https://doi.org/https://doi.org/10.1029/2001JD000807>
- Bindle, L., Martin, R. V., Cooper, M. J., Lundgren, E. W., Eastham, S. D., Auer, B. M., Clune, T. L., Weng, H., Lin, J., Murray, L. T., Meng, J., Keller, C. A., Putman, W. M., Pawson, S., & Jacob, D. J. (2021). Grid-stretching capability for the GEOS-Chem 13.0.0 atmospheric chemistry model. *Geosci. Model Dev.*, 14(10), 5977-5997. <https://doi.org/10.5194/gmd-14-5977-2021>
- Bonilla, E., Mickley, L. J., Raheja, G., Eastham, S. D., Buonocore, J., Alencar, A., Verchot, L., Westervelt, D., & Castro, M. C. (2023). Health impacts of smoke exposure in South America: increased risk for populations in the Amazonian Indigenous territories. *Environmental Research: Health*, 1(2), 021007.
- Burnett, R., Chen, H., Szyszkowicz, M., Fann, N., Hubbell, B., Pope, C. A., Apte, J. S., Brauer, M., Cohen, A., Weichenthal, S., Coggins, J., Di, Q., Brunekreef, B., Frostad, J., Lim, S. S., Kan, H., Walker, K. D., Thurston, G. D., Hayes, R. B., Lim, C. C., Turner, M. C., Jerrett, M., Krewski, D., Gapstur, S. M., Diver, W. R., Ostro, B., Goldberg, D., Crouse, D.



- 580 L., Martin, R. V., Peters, P., Pinault, L., Tjepkema, M., van Donkelaar, A., Villeneuve, P. J., Miller, A. B., Yin, P.,
Zhou, M., Wang, L., Janssen, N. A. H., Marra, M., Atkinson, R. W., Tsang, H., Quoc Thach, T., Cannon, J. B., Allen,
R. T., Hart, J. E., Laden, F., Cesaroni, G., Forastiere, F., Weinmayr, G., Jaensch, A., Nagel, G., Concini, H., & Spadaro,
J. V. (2018). Global estimates of mortality associated with long-term exposure to outdoor fine particulate matter.
Proceedings of the National Academy of Sciences, 115(38), 9592-9597. <https://doi.org/10.1073/pnas.1803222115>
- 585 Butt, E. W., Conibear, L., Knote, C., & Spracklen, D. V. (2021). Large Air Quality and Public Health Impacts due to
Amazonian Deforestation Fires in 2019. *GeoHealth*, 5(7), e2021GH000429.
<https://doi.org/https://doi.org/10.1029/2021GH000429>
- Butt, E. W., Conibear, L., Reddington, C. L., Darbyshire, E., Morgan, W. T., Coe, H., Artaxo, P., Brito, J., Knote, C., &
Spracklen, D. V. (2020). Large air quality and human health impacts due to Amazon forest and vegetation fires.
590 *Environmental Research Communications*, 2(9), 095001. <https://doi.org/10.1088/2515-7620/abb0db>
- Byard, R. W. (2019). Carbon monoxide – the silent killer. *Forensic Science, Medicine and Pathology*, 15(1), 1-2.
<https://doi.org/10.1007/s12024-018-0040-5>
- Cammelli, F., Garrett, R. D., Barlow, J., & Parry, L. (2020). Fire risk perpetuates poverty and fire use among Amazonian
smallholders. *Global Environmental Change*, 63, 102096.
- 595 Center for International Earth Science Information Network, C. C. U. (2018). *Gridded Population of the World, Version 4
(GPWv4): Basic Demographic Characteristics, Revision 11* NASA Socioeconomic Data and Applications Center
(SEDAC). <https://doi.org/10.7927/H46M34XX>
- Cobelo, I., Castelhan, F. J., Borge, R., Roig, H. L., Adams, M., Amini, H., Koutrakis, P., & Réquia, W. J. (2023). The impact
of wildfires on air pollution and health across land use categories in Brazil over a 16-year period. *Environmental*
600 *Research*, 224, 115522.
- Cochrane, M. A. (2003). Fire science for rainforests. *Nature*, 421(6926), 913-919. <https://doi.org/10.1038/nature01437>
- Covey, K., Soper, F., Pangala, S., Bernardino, A., Pagliaro, Z., Basso, L., Cassol, H., Fearnside, P., Navarrete, D., Novoa, S.,
Sawakuchi, H., Lovejoy, T., Marengo, J., Peres, C. A., Baillie, J., Bernasconi, P., Camargo, J., Freitas, C., Hoffman,
B., Nardoto, G. B., Nobre, I., Mayorga, J., Mesquita, R., Pavan, S., Pinto, F., Rocha, F., de Assis Mello, R., Thuault,
605 A., Bahl, A. A., & Elmore, A. (2021). Carbon and Beyond: The Biogeochemistry of Climate in a Rapidly Changing
Amazon [Review]. *Frontiers in Forests and Global Change*, 4. <https://doi.org/10.3389/ffgc.2021.618401>
- da Cruz, D. C., Benayas, J. M. R., Ferreira, G. C., Santos, S. R., & Schwartz, G. (2021). An overview of forest loss and
restoration in the Brazilian Amazon. *New Forests*, 52, 1-16.
- de Moura, F. R., Machado, P. D. W., Ramires, P. F., Tavella, R. A., Carvalho, H., & da Silva Júnior, F. M. R. (2024). In the
610 line of fire: Analyzing burning impacts on air pollution and air quality in an Amazonian city, Brazil. *Atmospheric
Pollution Research*, 15(4), 102033.
- Eastham, S. D., Long, M. S., Keller, C. A., Lundgren, E., Yantosca, R. M., Zhuang, J., Li, C., Lee, C. J., Yannetti, M., Auer,
B. M., Clune, T. L., Kouatchou, J., Putman, W. M., Thompson, M. A., Trayanov, A. L., Molod, A. M., Martin, R. V.,
& Jacob, D. J. (2018). GEOS-Chem High Performance (GCHP v11-02c): a next-generation implementation of the
615 GEOS-Chem chemical transport model for massively parallel applications. *Geosci. Model Dev.*, 11(7), 2941-2953.
<https://doi.org/10.5194/gmd-11-2941-2018>
- Elakiya, N., Keerthana, G., & Safiya, S. (2023). Effects of Forest Fire on Soil Properties. *International Journal of Plant & Soil
Science*, 35(20), 8-17.
- Espinoza, J.-C., Jimenez, J. C., Marengo, J. A., Schongart, J., Ronchail, J., Lavado-Casimiro, W., & Ribeiro, J. V. M. (2024).
620 The new record of drought and warmth in the Amazon in 2023 related to regional and global climatic features.
Scientific Reports, 14(1), 8107.
- F. G. Assis, L. F., Ferreira, K. R., Vinhas, L., Maurano, L., Almeida, C., Carvalho, A., Rodrigues, J., Maciel, A., & Camargo,
C. (2019). TerraBrasilis: A Spatial Data Analytics Infrastructure for Large-Scale Thematic Mapping. *ISPRS
International Journal of Geo-Information*, 8(11).
- 625 Feldpausch, T. R., Phillips, O. L., Brienen, R. J. W., Gloor, E., Lloyd, J., Lopez-Gonzalez, G., Monteagudo-Mendoza, A.,
Malhi, Y., Alarcón, A., Álvarez Dávila, E., Alvarez-Loayza, P., Andrade, A., Aragao, L. E. O. C., Arroyo, L., Aymard
C, G. A., Baker, T. R., Baraloto, C., Barroso, J., Bonal, D., Castro, W., Chama, V., Chave, J., Domingues, T. F.,
Fauset, S., Groot, N., Honorio Coronado, E., Laurance, S., Laurance, W. F., Lewis, S. L., Licona, J. C., Marimon, B.
S., Marimon-Junior, B. H., Mendoza Bautista, C., Neill, D. A., Oliveira, E. A., Oliveira dos Santos, C., Pallqui



- 630 Camacho, N. C., Pardo-Molina, G., Prieto, A., Quesada, C. A., Ramírez, F., Ramírez-Angulo, H., Réjou-Méchain, M., Rudas, A., Saiz, G., Salomão, R. P., Silva-Espejo, J. E., Silveira, M., ter Steege, H., Stropp, J., Terborgh, J., Thomas-Caesar, R., van der Heijden, G. M. F., Vásquez Martínez, R., Vilanova, E., & Vos, V. A. (2016). Amazon forest response to repeated droughts. *Global Biogeochemical Cycles*, 30(7), 964-982. <https://doi.org/https://doi.org/10.1002/2015GB005133>
- 635 Fuentes-Ramirez, A., Almonacid-Muñoz, L., Muñoz-Gómez, N., & Moloney, K. A. (2022). Spatio-temporal variation in soil nutrients and plant recovery across a fire-severity gradient in old-growth araucaria-Nothofagus forests of south-Central Chile. *Forests*, 13(3), 448.
- Gatti, L. V., Basso, L. S., Miller, J. B., Gloor, M., Gatti Domingues, L., Cassol, H. L. G., Tejada, G., Aragão, L. E. O. C., Nobre, C., Peters, W., Marani, L., Arai, E., Sanches, A. H., Corrêa, S. M., Anderson, L., Von Randow, C., Correia, C. S. C., Crispim, S. P., & Neves, R. A. L. (2021). Amazonia as a carbon source linked to deforestation and climate change. *Nature*, 595(7867), 388-393. <https://doi.org/10.1038/s41586-021-03629-6>
- 640 Gaudel, A., Cooper, O. R., Ancellet, G., Barret, B., Boynard, A., Burrows, J. P., Clerbaux, C., Coheur, P. F., Cuesta, J., Cuevas, E., Doniki, S., Dufour, G., Ebojje, F., Foret, G., Garcia, O., Granados-Muñoz, M. J., Hannigan, J. W., Hase, F., Hassler, B., Huang, G., Hurtmans, D., Jaffe, D., Jones, N., Kalabokas, P., Kerridge, B., Kulawik, S., Latter, B., Leblanc, T., Le Flochmoën, E., Lin, W., Liu, J., Liu, X., Mahieu, E., McClure-Begley, A., Neu, J. L., Osman, M., Palm, M., Petetin, H., Petropavlovskikh, I., Querel, R., Rahpoe, N., Rozanov, A., Schultz, M. G., Schwab, J., Siddans, R., Smale, D., Steinbacher, M., Tanimoto, H., Tarasick, D. W., Thouret, V., Thompson, A. M., Trickl, T., Weatherhead, E., Wespes, C., Worden, H. M., Vigouroux, C., Xu, X., Zeng, G., & Ziemke, J. (2018). Tropospheric Ozone Assessment Report: Present-day distribution and trends of tropospheric ozone relevant to climate and global atmospheric chemistry model evaluation. *Elementa: Science of the Anthropocene*, 6, 39. <https://doi.org/10.1525/elementa.291>
- 645 Gelaro, R., McCarty, W., Suárez, M. J., Todling, R., Molod, A., Takacs, L., Randles, C. A., Darmenov, A., Bosilovich, M. G., Reichle, R., Wargan, K., Coy, L., Cullather, R., Draper, C., Akella, S., Buchard, V., Conaty, A., da Silva, A. M., Gu, W., Kim, G.-K., Koster, R., Lucchesi, R., Merkova, D., Nielsen, J. E., Partyka, G., Pawson, S., Putman, W., Rienecker, M., Schubert, S. D., Sienkiewicz, M., & Zhao, B. (2017). The Modern-Era Retrospective Analysis for Research and Applications, Version 2 (MERRA-2). *Journal of Climate*, 30(14), 5419-5454. <https://doi.org/https://doi.org/10.1175/JCLI-D-16-0758.1>
- 650 Godar, J., Gardner, T. A., Tizado, E. J., & Pacheco, P. (2014). Actor-specific contributions to the deforestation slowdown in the Brazilian Amazon. *Proceedings of the National Academy of Sciences*, 111(43), 15591-15596. <https://doi.org/10.1073/pnas.1322825111>
- 660 Gonzalez-Alonso, L., Val Martin, M., & Kahn, R. A. (2019). Biomass-burning smoke heights over the Amazon observed from space. *Atmospheric Chemistry and Physics*, 19(3), 1685-1702.
- Guenther, A. B., Jiang, X., Heald, C. L., Sakulyanontvittaya, T., Duhl, T., Emmons, L. K., & Wang, X. (2012). The Model of Emissions of Gases and Aerosols from Nature version 2.1 (MEGAN2.1): an extended and updated framework for modeling biogenic emissions. *Geosci. Model Dev.*, 5(6), 1471-1492. <https://doi.org/10.5194/gmd-5-1471-2012>
- 665 Harris, L. M., Lin, S.-J., & Tu, C. (2016). High-Resolution Climate Simulations Using GFDL HiRAM with a Stretched Global Grid. *Journal of Climate*, 29(11), 4293-4314. <https://doi.org/https://doi.org/10.1175/JCLI-D-15-0389.1>
- Hill, C., DeLuca, C., Balaji, Suarez, M., & Silva, A. D. (2004). The architecture of the Earth System Modeling Framework. *Computing in Science & Engineering*, 6(1), 18-28. <https://doi.org/10.1109/MCISE.2004.1255817>
- 670 Jacobson, M. Z. (2014). Effects of biomass burning on climate, accounting for heat and moisture fluxes, black and brown carbon, and cloud absorption effects. *Journal of Geophysical Research: Atmospheres*, 119(14), 8980-9002. <https://doi.org/https://doi.org/10.1002/2014JD021861>
- Jaffe, D. A., Schnieder, B., & Inouye, D. (2022). Use of PM 2.5 to CO ratio as a tracer of wildfire smoke in urban areas. *Atmospheric Chemistry & Physics Discussions*.
- 675 Jerrett, M., Burnett, R. T., Beckerman, B. S., Turner, M. C., Krewski, D., Thurston, G., Martin, R. V., van Donkelaar, A., Hughes, E., & Shi, Y. (2013). Spatial analysis of air pollution and mortality in California. *American journal of respiratory and critical care medicine*, 188(5), 593-599.
- Jerrett, M., Burnett, R. T., Pope III, C. A., Ito, K., Thurston, G., Krewski, D., Shi, Y., Calle, E., & Thun, M. (2009). Long-term ozone exposure and mortality. *New England Journal of Medicine*, 360(11), 1085-1095.



- 680 Jiang, Y., Yang, X.-Q., Liu, X., Qian, Y., Zhang, K., Wang, M., Li, F., Wang, Y., & Lu, Z. (2020). Impacts of wildfire aerosols on global energy budget and climate: The role of climate feedbacks. *Journal of Climate*, 33(8), 3351-3366.
- Jiménez-Muñoz, J. C., Mattar, C., Barichivich, J., Santamaría-Artigas, A., Takahashi, K., Malhi, Y., Sobrino, J. A., & Schrier, G. v. d. (2016). Record-breaking warming and extreme drought in the Amazon rainforest during the course of El Niño 2015–2016. *Scientific Reports*, 6(1), 33130. <https://doi.org/10.1038/srep33130>
- 685 Keeley, J. E., Bond, W. J., Bradstock, R. A., Pausas, J. G., & Rundel, P. W. (2011). *Fire in Mediterranean ecosystems: ecology, evolution and management*. Cambridge University Press.
- Kelly, F. J., & Fussell, J. C. (2015). Air pollution and public health: emerging hazards and improved understanding of risk. *Environmental Geochemistry and Health*, 37(4), 631-649. <https://doi.org/10.1007/s10653-015-9720-1>
- 690 Liang, F., Liu, F., Huang, K., Yang, X., Li, J., Xiao, Q., Chen, J., Liu, X., Cao, J., Shen, C., Yu, L., Lu, F., Wu, X., Wu, X., Li, Y., Hu, D., Huang, J., Liu, Y., Lu, X., & Gu, D. (2020). Long-Term Exposure to Fine Particulate Matter and Cardiovascular Disease in China. *Journal of the American College of Cardiology*, 75(7), 707-717. <https://doi.org/10.1016/j.jacc.2019.12.031>
- Lin, H., Jacob, D. J., Lundgren, E. W., Sulprizio, M. P., Keller, C. A., Fritz, T. M., Eastham, S. D., Emmons, L. K., Campbell, P. C., Baker, B., Saylor, R. D., & Montuoro, R. (2021). Harmonized Emissions Component (HEMCO) 3.0 as a versatile emissions component for atmospheric models: application in the GEOS-Chem, NASA GEOS, WRF-GC, CESM2, NOAA GEFS-Aerosol, and NOAA UFS models. *Geosci. Model Dev.*, 14(9), 5487-5506. <https://doi.org/10.5194/gmd-14-5487-2021>
- 695 Liu, S., McVicar, T. R., Wu, X., Cao, X., & Liu, Y. (2024). Assessing the relative importance of dry-season incoming solar radiation and water storage dynamics during the 2005, 2010 and 2015 southern Amazon droughts: not all droughts are created equal. *Environmental Research Letters*, 19(3), 034027.
- 700 Liu, T., Mickley, L. J., Marlier, M. E., DeFries, R. S., Khan, M. F., Latif, M. T., & Karambelas, A. (2020). Diagnosing spatial biases and uncertainties in global fire emissions inventories: Indonesia as regional case study. *Remote Sensing of Environment*, 237, 111557. <https://doi.org/https://doi.org/10.1016/j.rse.2019.111557>
- 705 Malley, C. S., Henze, D. K., Kuylenstierna, J. C., Vallack, H. W., Davila, Y., Anenberg, S. C., Turner, M. C., & Ashmore, M. R. (2017). Updated global estimates of respiratory mortality in adults ≥ 30 years of age attributable to long-term ozone exposure. *Environmental Health Perspectives*, 125(8), 087021.
- Marengo, J. A., Tomasella, J., Alves, L. M., Soares, W. R., & Rodriguez, D. A. (2011). The drought of 2010 in the context of historical droughts in the Amazon region. *Geophysical Research Letters*, 38(12). <https://doi.org/https://doi.org/10.1029/2011GL047436>
- 710 Marlier, M. E., Bonilla, E. X., & Mickley, L. J. (2020). How Do Brazilian Fires Affect Air Pollution and Public Health? *GeoHealth*, 4(12), e2020GH000331. <https://doi.org/https://doi.org/10.1029/2020GH000331>
- Martin, R. V., Eastham, S. D., Bindle, L., Lundgren, E. W., Clune, T. L., Keller, C. A., Downs, W., Zhang, D., Lucchesi, R. A., Sulprizio, M. P., Yantosca, R. M., Li, Y., Estrada, L., Putman, W. M., Auer, B. M., Trayanov, A. L., Pawson, S., & Jacob, D. J. (2022). Improved advection, resolution, performance, and community access in the new generation (version 13) of the high-performance GEOS-Chem global atmospheric chemistry model (GCHP). *Geosci. Model Dev.*, 15(23), 8731-8748. <https://doi.org/10.5194/gmd-15-8731-2022>
- 715 Mataveli, G. A., de Oliveira, G., Seixas, H. T., Pereira, G., Stark, S. C., Gatti, L. V., Basso, L. S., Tejada, G., Cassol, H. L., & Anderson, L. O. (2021). Relationship between biomass burning emissions and deforestation in Amazonia over the last two decades. *Forests*, 12(9), 1217.
- 720 McDuffie, E. E., Smith, S. J., O'Rourke, P., Tibrewal, K., Venkataraman, C., Marais, E. A., Zheng, B., Crippa, M., Brauer, M., & Martin, R. V. (2020). A global anthropogenic emission inventory of atmospheric pollutants from sector- and fuel-specific sources (1970–2017): an application of the Community Emissions Data System (CEDS). *Earth Syst. Sci. Data*, 12(4), 3413-3442. <https://doi.org/10.5194/essd-12-3413-2020>
- 725 McGregor, S., Timmermann, A., Stuecker, M. F., England, M. H., Merrifield, M., Jin, F.-F., & Chikamoto, Y. (2014). Recent Walker circulation strengthening and Pacific cooling amplified by Atlantic warming. *Nature Climate Change*, 4(10), 888-892. <https://doi.org/10.1038/nclimate2330>
- Miranda, V. F., Albuquerque, R., Geirinhas, J., Peres, L. F., Libonati, R., Jimenez, J. C., & Trigo, I. F. (2026). Satellite-based land surface temperature and soil moisture observed during the 2023–2024 drought–heatwave events in the Amazon Basin. *Environmental Research: Climate*, 5(1), 015012.



- 730 Nawaz, M., & Henze, D. (2020). Premature deaths in Brazil associated with long-term exposure to PM_{2.5} from Amazon fires between 2016 and 2019. *GeoHealth*, 4(8), e2020GH000268.
- Nepstad, D., Lefebvre, P., Lopes da Silva, U., Tomasella, J., Schlesinger, P., Solórzano, L., Moutinho, P., Ray, D., & Guerreira Benito, J. (2004). Amazon drought and its implications for forest flammability and tree growth: a basin-wide analysis. *Global Change Biology*, 10(5), 704-717. <https://doi.org/https://doi.org/10.1111/j.1529-8817.2003.00772.x>
- 735 New, T. R. (2014). *Insects, fire and conservation*. Springer.
- Papastefanou, P., Zang, C. S., Angelov, Z., De Castro, A. A., Jimenez, J. C., De Rezende, L. F. C., Ruscica, R. C., Sakschewski, B., Sörensson, A. A., & Thonicke, K. (2022). Recent extreme drought events in the Amazon rainforest: Assessment of different precipitation and evapotranspiration datasets and drought indicators. *Biogeosciences*, 19(16), 3843-3861.
- Pausas, J. G., & Keeley, J. E. (2019). Wildfires as an ecosystem service. *Frontiers in Ecology and the Environment*, 17(5), 289-295.
- 740 Permar, W., Wang, Q., Selimovic, V., Wielgasz, C., Yokelson, R. J., Hornbrook, R. S., Hills, A. J., Apel, E. C., Ku, I. T., & Zhou, Y. (2021). Emissions of trace organic gases from Western US wildfires based on WE-CAN aircraft measurements. *Journal of Geophysical Research: Atmospheres*, 126(11), e2020JD033838.
- Pfleger, E., Adrian, C., Lutz, R., & Drexler, H. (2023). Science communication on the public health risks of air pollution: a computational scoping review from 1958 to 2022. *Archives of Public Health*, 81(1), 14. <https://doi.org/10.1186/s13690-023-01031-4>
- 745 Pope, C. A., Ezzati, M., Cannon, J. B., Allen, R. T., Jerrett, M., & Burnett, R. T. (2018). Mortality risk and PM_{2.5} air pollution in the USA: an analysis of a national prospective cohort. *Air Quality, Atmosphere & Health*, 11(3), 245-252. <https://doi.org/10.1007/s11869-017-0535-3>
- 750 Prodes, I. P. (2013). Monitoramento da floresta Amazônica Brasileira por satélite. *Inst. Nac. De Pesqui. Espac. Proj. Prodes*, 25, 2013.
- Puett Robin, C., Hart Jaime, E., Suh, H., Mittleman, M., & Laden, F. (2011). Particulate Matter Exposures, Mortality, and Cardiovascular Disease in the Health Professionals Follow-up Study. *Environmental Health Perspectives*, 119(8), 1130-1135. <https://doi.org/10.1289/ehp.1002921>
- 755 Randerson, J., Van Der Werf, G., Giglio, L., Collatz, G., & Kasibhatla, P. (2018). Global Fire Emissions Database, Version 4.1 (GFEDv4), ORNL DAAC, Oak Ridge, Tennessee, USA. In: 0.3334/ORNLDAAC/1293.
- Regan, H. M., Keith, D. A., Regan, T. J., Tozer, M. G., & Tootell, N. (2011). Fire management to combat disease: turning interactions between threats into conservation management. *Oecologia*, 167, 873-882.
- Rosan, T. M., Sitch, S., O'sullivan, M., Basso, L. S., Wilson, C., Silva, C., Gloor, E., Fawcett, D., Heinrich, V., & Souza, J. G. (2024). Synthesis of the land carbon fluxes of the Amazon region between 2010 and 2020. *Communications Earth & Environment*, 5(1), 46.
- 760 Scholes, R. J., Archibald, S., & von MALTITZ, G. (2011). Emissions from fire in Sub-Saharan Africa: the magnitude of sources, their variability and uncertainty. *Global Environmental Research*, 15(1), 53-63.
- Seltzer, K. M., Shindell, D. T., & Malley, C. S. (2018). Measurement-based assessment of health burdens from long-term ozone exposure in the United States, Europe, and China. *Environmental Research Letters*, 13(10), 104018. <https://doi.org/10.1088/1748-9326/aae29d>
- 765 Shen, S., Li, C., van Donkelaar, A., Jacobs, N., Wang, C., & Martin, R. V. (2024). Enhancing Global Estimation of Fine Particulate Matter Concentrations by Including Geophysical a Priori Information in Deep Learning. *ACS ES&T Air*, 1(5), 332-345. <https://doi.org/10.1021/acsestair.3c00054>
- 770 Silva Junior, C. H. L., Anderson, L. O., Silva, A. L., Almeida, C. T., Dalagnol, R., Pletsch, M. A. J. S., Penha, T. V., Paloschi, R. A., & Aragão, L. E. O. C. (2019). Fire Responses to the 2010 and 2015/2016 Amazonian Droughts [Original Research]. *Frontiers in Earth Science*, 7. <https://doi.org/10.3389/feart.2019.00097>
- Staal, A., Flores, B. M., Aguiar, A. P. D., Bosmans, J. H. C., Fetzner, I., & Tuinenburg, O. A. (2020). Feedback between drought and deforestation in the Amazon. *Environmental Research Letters*, 15(4), 044024. <https://doi.org/10.1088/1748-9326/ab738e>
- 775 Suarez, M., Trayanov, A., Hill, C., Schopf, P., & Vikhliayev, Y. (2007). MAPL: a high-level programming paradigm to support more rapid and robust encoding of hierarchical trees of interacting high-performance components. Proceedings of the 2007 symposium on Component and framework technology in high-performance and scientific computing,



- 780 Sun, J., & Zhou, T. (2017). Health risk assessment of China's main air pollutants. *BMC Public Health*, 17(1), 212.
<https://doi.org/10.1186/s12889-017-4130-1>
- Turner, M. C., Jerrett, M., Pope III, C. A., Krewski, D., Gapstur, S. M., Diver, W. R., Beckerman, B. S., Marshall, J. D., Su,
J., & Crouse, D. L. (2016). Long-term ozone exposure and mortality in a large prospective study. *American journal
of respiratory and critical care medicine*, 193(10), 1134-1142.
- 785 van der Laan-Luijkx, I. T., van der Velde, I. R., Krol, M. C., Gatti, L. V., Domingues, L. G., Correia, C. S. C., Miller, J. B.,
Gloor, M., van Leeuwen, T. T., Kaiser, J. W., Wiedinmyer, C., Basu, S., Clerbaux, C., & Peters, W. (2015). Response
of the Amazon carbon balance to the 2010 drought derived with CarbonTracker South America. *Global
Biogeochemical Cycles*, 29(7), 1092-1108. <https://doi.org/https://doi.org/10.1002/2014GB005082>
- van der Werf, G. R., Randerson, J. T., Giglio, L., van Leeuwen, T. T., Chen, Y., Rogers, B. M., Mu, M., van Marle, M. J. E.,
Morton, D. C., Collatz, G. J., Yokelson, R. J., & Kasibhatla, P. S. (2017). Global fire emissions estimates during
790 1997–2016. *Earth Syst. Sci. Data*, 9(2), 697-720. <https://doi.org/10.5194/essd-9-697-2017>
- van Leeuwen, T. T., van der Werf, G. R., Hoffmann, A. A., Detmers, R. G., Rücker, G., French, N. H. F., Archibald, S.,
Carvalho Jr, J. A., Cook, G. D., de Groot, W. J., Hély, C., Kasischke, E. S., Kloster, S., McCarty, J. L., Pettinari, M.
L., Savadogo, P., Alvarado, E. C., Boschetti, L., Manuri, S., Meyer, C. P., Siegert, F., Trollope, L. A., & Trollope,
W. S. W. (2014). Biomass burning fuel consumption rates: a field measurement database. *Biogeosciences*, 11(24),
795 7305-7329. <https://doi.org/10.5194/bg-11-7305-2014>
- van Marle, M. J. E., Field, R. D., van der Werf, G. R., Estrada de Wagt, I. A., Houghton, R. A., Rizzo, L. V., Artaxo, P., &
Tsigaridis, K. (2017). Fire and deforestation dynamics in Amazonia (1973–2014). *Global Biogeochemical Cycles*,
31(1), 24-38. <https://doi.org/https://doi.org/10.1002/2016GB005445>
- Vicente-Serrano, S. M., Beguería, S., & López-Moreno, J. I. (2010). A multiscalar drought index sensitive to global warming:
800 the standardized precipitation evapotranspiration index. *Journal of Climate*, 23(7), 1696-1718.
- Vodonos, A., Awad, Y. A., & Schwartz, J. (2018). The concentration-response between long-term PM_{2.5} exposure and
mortality; A meta-regression approach. *Environmental Research*, 166, 677-689.
- Vohra, K., Vodonos, A., Schwartz, J., Marais, E. A., Sulprizio, M. P., & Mickley, L. J. (2021). Global mortality from outdoor
fine particle pollution generated by fossil fuel combustion: Results from GEOS-Chem. *Environmental Research*, 195,
805 110754. <https://doi.org/https://doi.org/10.1016/j.envres.2021.110754>
- Ward, D. S., Kloster, S., Mahowald, N., Rogers, B., Randerson, J., & Hess, P. (2012). The changing radiative forcing of fires:
global model estimates for past, present and future. *Atmospheric Chemistry and Physics*, 12(22), 10857-10886.
- Werth, D., & Avissar, R. (2002). The local and global effects of Amazon deforestation. *Journal of Geophysical Research:
Atmospheres*, 107(D20), LBA 55-51-LBA 55-58. <https://doi.org/https://doi.org/10.1029/2001JD000717>
- 810 Wong Chit, M., Lai Hak, K., Tsang, H., Thach Thuan, Q., Thomas, G. N., Lam Kin Bong, H., Chan King, P., Yang, L., Lau
Alexis, K. H., Ayres Jon, G., Lee Siu, Y., Man Chan, W., Hedley Anthony, J., & Lam Tai, H. (2015). Satellite-Based
Estimates of Long-Term Exposure to Fine Particles and Association with Mortality in Elderly Hong Kong Residents.
Environmental Health Perspectives, 123(11), 1167-1172. <https://doi.org/10.1289/ehp.1408264>
- Xu, X., Jia, G., Zhang, X., Riley, W. J., & Xue, Y. (2020). Climate regime shift and forest loss amplify fire in Amazonian
815 forests. *Global Change Biology*, 26(10), 5874-5885.
- Yang, W., & Omaye, S. T. (2009). Air pollutants, oxidative stress and human health. *Mutation Research/Genetic Toxicology
and Environmental Mutagenesis*, 674(1), 45-54. <https://doi.org/https://doi.org/10.1016/j.mrgentox.2008.10.005>
- Zhu, L., Val Martin, M., Gatti, L. V., Kahn, R., Hecobian, A., & Fischer, E. V. (2018). Development and implementation of a
new biomass burning emissions injection height scheme (BBEIH v1. 0) for the GEOS-Chem model (v9-01-01).
820 *Geoscientific Model Development*, 11(10), 4103-4116.
- Zu, K., Shi, L., Prueitt, R. L., Liu, X., & Goodman, J. E. (2018). Critical review of long-term ozone exposure and asthma
development. *Inhalation Toxicology*, 30(3), 99-113. <https://doi.org/10.1080/08958378.2018.1455772>